

Title	Lateral Tension-Induced Penetration of Particles into a Liposome
Author(s)	Shigyou, Kazuki; Nagai, Ken H.; Hamada, Tsutomu
Citation	Materials, 10(7): 765
Issue Date	2017-07-07
Type	Journal Article
Text version	publisher
URL	http://hdl.handle.net/10119/15286
Rights	Materials 2017, 10(7), 765; doi:10.3390/ma10070765 This is an open access article distributed under the Creative Commons Attribution License which permits unrestricted use, distribution, and reproduction in any medium, provided the original work is properly cited. (CC BY 4.0).
Description	

Communication

Lateral Tension-Induced Penetration of Particles into a Liposome

Kazuki Shigyou ^{1,2}, Ken H. Nagai ^{1,*}  and Tsutomu Hamada ^{1,*}

¹ School of Materials Science, Japan Advanced Institute of Science and Technology, 1-1 Asahidai, Nomi, Ishikawa 923-1292, Japan; s1440007@jaist.ac.jp

² Bio-AFM Frontier Research Center, Institute of Science and Engineering, Kanazawa University, Kakuma-machi, Kanazawa 920-1192, Japan

* Correspondence: k-nagai@jaist.ac.jp (K.H.N.); t-hamada@jaist.ac.jp (T.H.); Tel.: +81-761-51-1672 (K.H.N.); +81-761-51-1670 (T.H.)

Received: 8 May 2017; Accepted: 4 July 2017; Published: 7 July 2017

Abstract: It is important that we understand the mechanism of the penetration of particles into a living cell to achieve advances in bionanotechnology, such as for treatment, visualization within a cell, and genetic modification. Although there have been many studies on the application of functional particles to cells, the basic mechanism of penetration across a biological membrane is still poorly understood. Here we used a model membrane system to demonstrate that lateral membrane tension drives particle penetration across a lipid bilayer. After the application of osmotic pressure, fully wrapped particles on a liposome surface were found to enter the liposome. We discuss the mechanism of the tension-induced penetration in terms of narrow constriction of the membrane at the neck part. The present findings are expected to provide insight into the application of particles to biological systems.

Keywords: particle penetration; lateral tension; lipid membrane; gene delivery method

1. Introduction

Nano/submicron particles have been actively studied because of their potential for controlling living cells, such as for drug delivery [1–5], local heating [6], and the visualization of proteins [7]. To express these functions, particles need to be transported into cells, and this process normally involves cellular uptake functions that are controlled by proteins [8]. Cells wrap particles within their membranes, and membrane-wrapped particles then enter the cells through fission of the membrane.

Membrane fission in a living cell has been shown to be controlled by dynamin proteins, which induce bilayer constriction and lateral tension to achieve fission of the tube (see Figure 5 for a definition of “neck” and “tube”) [9–12]. These results imply that the application of lateral tension at a constricted bilayer can promote the penetration of particles through a membrane. We previously reported a high-efficiency particle penetration system that did not involve proteins, where the self-penetration of oxide carbon particles on artificial lipid vesicles was observed [13]. The particles tended to be wrapped by membranes when the particles strongly adhered to the membrane surface. Excess surface area of the membrane was then decreased to create wrapping regions. Due to the increase in lateral tension caused by the wrapping of numerous particles, the membrane could be cut at the neck region of fully wrapped particles.

In this study, we demonstrate particle penetration through a membrane induced by an increase in membrane lateral tension using a cell-sized liposome without the aid of proteins. Previously, we reported the preparation of liposomes with fully wrapped or partially wrapped particles with the use of centrifugal force [14]. In this experiment, we used fully wrapped particles. Lateral tension drives the release of wrapped particles from the mother liposome.

2. Results

First, we prepared liposomes with fully wrapped particles by applying centrifugal force to the mixture of liposomes and particles (the detailed procedure is indicated in the Materials and Methods section) [14]. Next, we observed the response of the particles to the application of lateral tension under a decrease of the sucrose concentration in the bulk solution (a video of this penetration is available in the SI). Figure 1a shows a phase-contrast image of wrapped particles on the liposome before the application of lateral tension. Each particle is indicated by a circle. After the application of lateral tension, the particles penetrated into the liposome (Figure 1b). In addition, an experiment with a fluorescent lipid shows that penetrated particles were covered by the membrane (Figure 2). This implies that the penetration was caused by membrane scission at the neck of a fully wrapped particle.

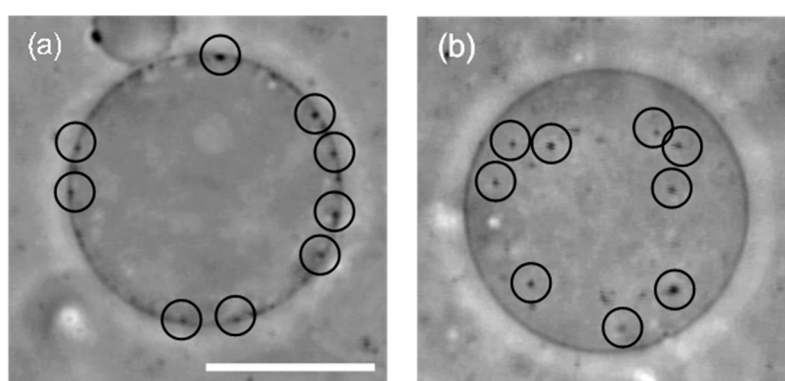


Figure 1. (a) A liposome with 200 nm fully wrapped particles before the application of osmotic pressure. Black circles show the position of fully wrapped particles; (b) Penetration of particles after the application of osmotic pressure. Scale bar is 10 μm .

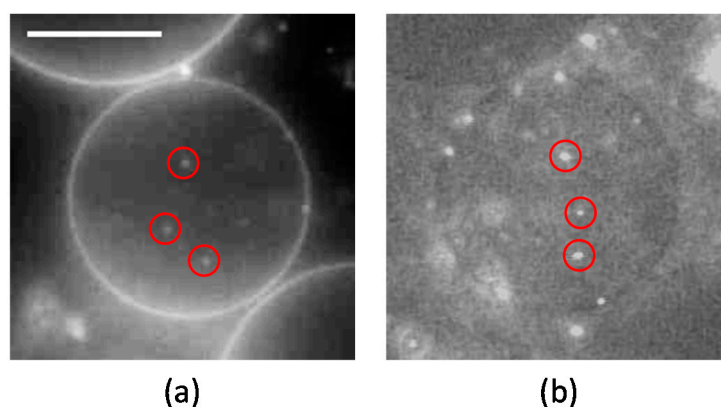


Figure 2. Microscopic images of (a) fluorescent lipid rho-DHPE (N-(rhodamine red-X)-1,2-dihexadecanoyl-sn-glycero-3-phosphoethanolamine triethylammonium salt) and (b) YG-particle fluorescence. The red circles indicate penetrated particles. Scale bar is 10 μm .

Next, we focused on the equatorial plane of the liposomes to observe the dynamic process of particle penetration. Figure 3 shows time-lapse images of the penetration of a wrapped particle under the application of lateral tension (calculation of the lateral tension is mentioned in the Materials and Methods section). Membrane fission occurred within 0.03 s. Notably, we did not observe any structural connection between the mother liposome and the penetrated particles after fission.

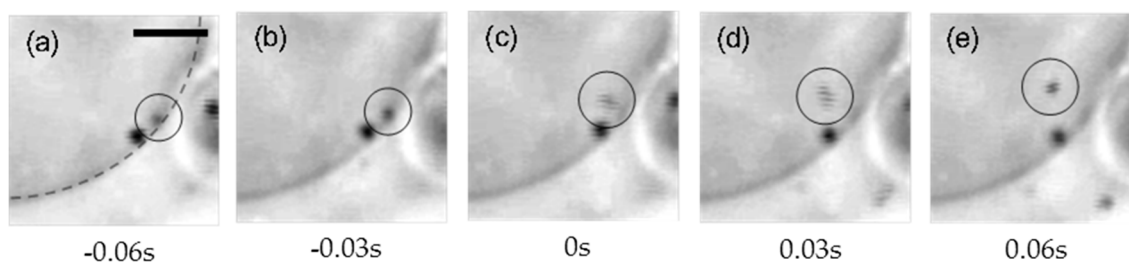


Figure 3. (a–e) Time-lapse images of the particle-uptake into a liposome (the time 0 s means the initiation of the particle penetration.). The black circle surrounds a 200 nm fully wrapped particle. The gray broken line shows the edge of the liposome. Scale bar is 10 μm .

We measured the time-dependent change in lateral tension and the particle penetration ratio for a single liposome (Figure 4). Membrane lateral tension was estimated by a change in the liposome surface area. Lateral tension increased just after the application of osmotic pressure at 0 to 250 s, and stayed between 0.02–0.03 N/m, as shown in Figure 4a. The temporary decrease in the tension at approximately 500 s may result from the formation of transient pores at the flat space of the membrane [15]. Conversely, the penetration ratio only began to increase 100 s after the increase in lateral tension, and became almost constant after 400 s (Figure 4b). We confirmed that all the liposomes with fully wrapped particles show the penetration when lateral tension of >0.01 N/m was applied ($N = 11$).

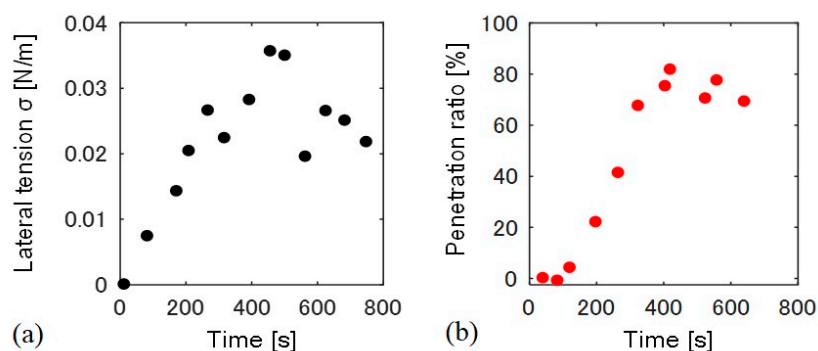


Figure 4. Time course of (a) lateral tension σ and (b) the particle penetration ratio. The time 0 s indicates the time at which hypo-osmotic solution was added to the liposome solution.

Next, we examined the dependence of penetration behavior on lateral tension. We applied several different osmotic pressures to induce different lateral tensions, and confirmed whether fully wrapped particles penetrated the membrane under five final osmotic pressures (Table 1). We determined six final lateral tensions (σ_f) 600 s after the application of osmotic pressure, because these tensions became almost constant at 600 s, as shown in Figure 4a. Note that the negative penetration ratio of 0.003 N/m is attributed from error of measurements. We determined the penetration ratio by counting the number of fully wrapped particles on the membrane surface and those penetrated into the liposome from sectional images (the detailed calculation is indicated in the Materials and Methods section). Fluctuation of those particle numbers results in the error of measurements.

Table 1. Relationship between the final lateral tension and penetration ratio.

Concentration Difference ΔC ($C_{\text{in}} - C_{\text{out}}$) (mM)	2.5	10	10	12.5	25	50
Lateral tension σ_f (N/m)	0.003	0.017	0.027	0.032	0.027	0.026
Penetration ratio (%)	−0.6	4.7	100	6.2	7.9	69

3. Discussion

The present results show that the application of lateral tension induces the penetration of fully wrapped particles into giant liposomes. The penetrated particles were covered by the membrane (as shown in Figure 2), which implies that the penetration was caused by membrane scission at the neck of a fully wrapped particle (Figure 5). Penetration was observed when applied lateral tension was over the order of 0.01 N/m (Table 1). Now we assume that the membrane neck consists of a tube structure with radius r_t , as in Figure 5. In Reference [16], the tube radius r_t is given by

$$r_t = \sqrt{\frac{K_b}{2\sigma}} \quad (1)$$

where we assumed, for simplicity, that the neck tube is driven by the force of particle adhesion.

K_b is bending modulus ($\sim 20 k_B T$, k_B is Boltzmann constant, T is room temperature) and σ is lateral tension. After the application of osmotic pressure, the tube radius decreased with increasing lateral tension. If we substitute $\sigma \sim 0.01$ N/m required to induce the particle penetration into Equation (1), $r_t \sim 2$ nm, which is shorter than bilayer thickness (~ 4 nm). Thus, when the tube radius is constricted to become close to bilayer thickness, the tube probably transitions into a hemi-fission state. Further increase in lateral tension would generate the scission of hemi-fission structure so that wrapped particles penetrate into the liposome. The process from constricted tube to hemi-fission has been reported with dynamin-mediated membrane fission, where the driving force of constriction is the polymerization of dynamin [9]. Although here we found that fully wrapped particles show penetration when lateral tension of >0.01 N/m was applied, there is dispersion of the penetration ratio with the tension value (Figure 1). Two possible factors can be considered. (1) Fully wrapped particles prepared by applying centrifugal force have some differences in membrane deformation degree at the connection to a mother liposome, although there is no apparent difference in their microscopic images. The subtle difference in the connection may affect the tension-induced instability of the membrane neck; (2) Liposomes may initially have some tension, because sucrose concentration inside liposomes is stochastically determined during the process of liposome formation. It is difficult to determine absolute membrane tension including the initial tension, and we used relative tension value deduced from a change in liposomal size after the application of osmotic pressure. The initially tensed liposomes probably show high penetration ratio.

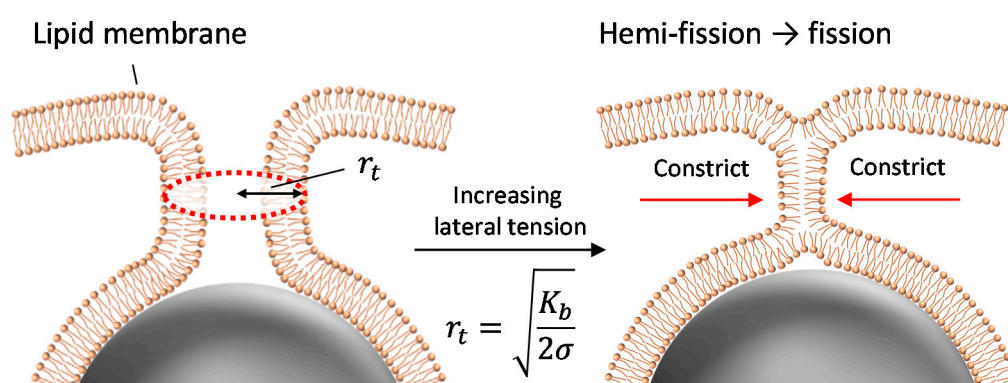


Figure 5. Schematic image of tube constriction and hemi-fission at the neck with increase in lateral tension.

4. Materials and Methods

DOPC (1,2-dioleoyl-*sn*-glycero-3-phosphocholine) was obtained from Avanti Polar Lipids (Alabaster, AL, USA). N-(rhodamine red-X)-1,2-dihexadecanoyl-*sn*-glycero-3-phosphoethanolamine triethylammonium salt (rho-DHPE) was obtained from Invitrogen (Waltham, MA, USA).

Surfactant-free YG fluorescent polystyrene particles with a radius of 200 nm were obtained from Polyscience (Warrington, PA, USA). Giant unilamellar vesicles were made by the electro-formation method [17] using 100 mM sucrose solution. Liposomes with fully wrapped particles were obtained as previously reported [14]. First, we prepared 5.0×10^{-3} g/L polystyrene particles with YG-fluorescence in 100 mM glucose solution for the adhesion of particles to the liposome. To remove the potential for including residual surfactants in the particle solution, the solution was centrifuged (20,685 RCF, 30 min), and the supernatant was replaced with deionized water. This procedure was repeated three times. The particles were then dispersed in 100 mM glucose solution. Second, we mixed 30 μ L liposome solution and 30 μ L particle solution, where the particles and liposomes are heavier than the outer solution. Finally, we applied 1600 RCF centrifugal forces to the mixture for 10 min and obtained fully wrapped particles that were associated with liposomes (a video of fully wrapped particles is available in the SI). The number of the liposomes with fully wrapped particles obtained in this procedure was 3–10 in 3 μ L.

To observe the dynamics of fully wrapped particles under lateral tension, we built a handmade chamber (Figure 6). First, we put a sample solution in the lower space of the chamber, and looked for membrane-associated particles within 5 min. Immediately after finding the liposomes, we focused on their equatorial plane to distinguish between fully wrapped and partially wrapped particles. Next, we filled the upper cylindrical space with 0 to 95 mM glucose solution to dilute the liposome solution, and placed a cover glass on the top. We then observed the liposome under the application of lateral tension for 20 min.

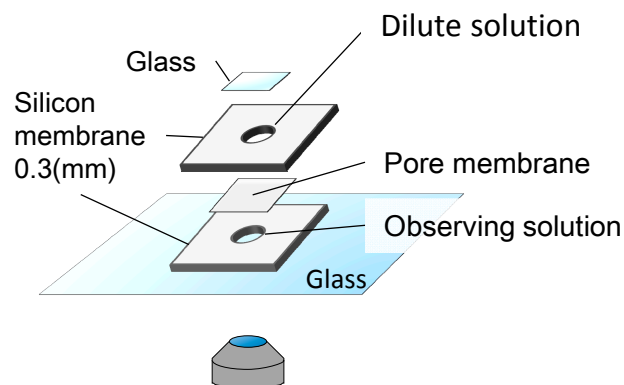


Figure 6. Schematic illustration of time-lapse observation under the application of tension.

To estimate lateral tension, we measured the radius of liposomes. The lateral tension can be calculated as

$$\sigma = K_a \left(\frac{\Delta S}{S_0} \right) \quad (2)$$

where $\Delta S = 4\pi R^2 - 4\pi R_0^2$ is the difference between the liposome surface area under osmotic pressure and the initial surface area (R_0 is the initial radius of a liposome and R is the radius of the liposome under osmotic pressure), $S_0 = 4\pi R_0^2$, and K_a is the membrane elastic modulus of DOPC (0.265 ± 18 N/m) [18]. To determine the penetration ratio, we counted the number of fully wrapped particles on the membrane surface and the number of particles that had penetrated into the liposome from sectional images using Image-J version 1.49o (National Institutes of Health, Bethesda, MD, USA). Figure 7 shows the region for counting the average number of fully wrapped particles N_{av}^{wrap} and the average number of penetrated particles N_{av}^{pe} in 2000 consecutive frames (60 s: the value was estimated

as $\Delta t = (\text{typical cross sectional area of liposomes}) / (\text{diffusion coefficient of 200 nm diameter particles})$, respectively. The total number of particles in one liposome, N^{wrap} and N^{pe} , are calculated as

$$\frac{N_{AV}^{pe}}{\pi R^2 h_{depth}} = \frac{N^{pe}}{\frac{4}{3} \pi R^3} \quad (3)$$

$$\frac{N_{AV}^{wrap}}{2\pi R h_{depth}} = \frac{N^{wrap}}{4\pi R^2} \quad (4)$$

The penetration ratio P is given by

$$P = \frac{N^{pe}(t + \Delta t) - N^{pe}(0)}{N^{wrap}(0)} \quad (5)$$

where t indicates the duration of the application of osmotic pressure, $N^{pe}(t + \Delta t)$ is the number of penetrated particles at time t during $\Delta t = 60$ s, $N^{pe}(0)$ is the number of penetrated particles before the application of lateral tension, $N^{wrap}(0)$ is the number of fully wrapped particles before the application of lateral tension, and h_{depth} is the depth of the focus ($h_{depth} \approx 400$ nm).

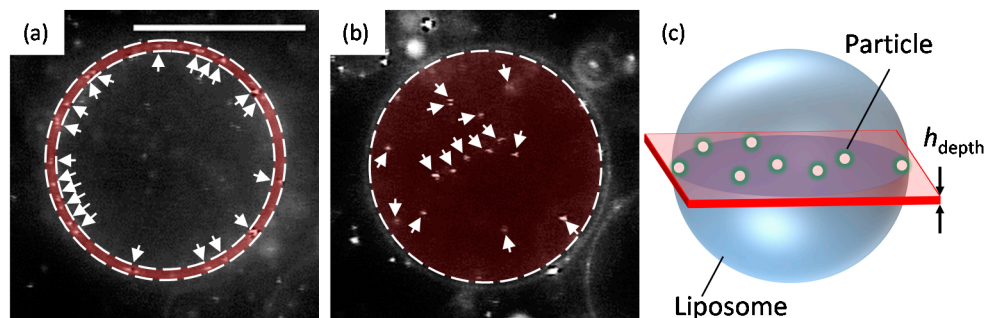


Figure 7. Regions for counting (a) fully wrapped particles and (b) penetrated particles. The white arrows indicate particles. Scale bar is 20 μm . (c) Schematic of the region observed by an optical microscope.

5. Conclusions

We prepared fully wrapped particles on a cell-sized liposome surface, and found that the particles entered the inner aqueous phase of the liposome under the application of lateral tension. The penetration was caused by tension-induced constriction of the neck part, which increases the probability of membrane hemi-fission. The scission of the hemi-fission leads to the detachment of fully wrapped particles. Our findings could lead to new technologies based on the mechanical properties of the membrane for transporting objects such as large plasmids and nanoparticles into a cell.

Supplementary Material

The following videos are available online at www.mdpi.com/1996-1944/10/7/765/s1, A video of fully wrapped particles on a membrane: Fully_wrapped_particles. A video of the process of penetration of fully wrapped particles under osmotic pressure: Penetration.

Acknowledgments: The authors are grateful for support from AMED-CREST, AMED, MEXT KAKENHI (Grant Nos. 15H00807 and 26103516 to T. H.), JSPS KAKENHI (Grant No. 15K12538 to T. H. and Grant No. 26610112 to K.H.N) and a SUNBOR SCHOLARSHIP from the SUNTORY FOUNDATION FOR LIFE SCIENCE. We thank Shunsuke F. Shimobayashi for useful suggestions.

Author Contributions: Kazuki Shigyuu and Ken H. Nagai designed the experiments; Kazuki Shigyuu performed the experiments; Kazuki Shigyuu analyzed the data; Kazuki Shigyuu wrote the manuscript, with revisions by Ken H. Nagai and Tsutomu Hamada.

Conflicts of Interest: The authors declare no conflict of interest.

References

1. Ting, C.; Wang, Z.-G. Interactions of a charged nanoparticle with a lipid membrane: Implications for gene delivery. *Biophys. J.* **2011**, *100*, 1288–1297. [[CrossRef](#)] [[PubMed](#)]
2. Majidi, S.; Sehrig, F.; Samiei, M.; Milani, M.; Abbasi, E.; Dadashzadeh, K.; Akbarzadeh, A. Magnetic nanoparticles: Applications in gene delivery and gene therapy. *Artif. Cells Nanomed. Biotechnol.* **2016**, *44*, 1186–1193. [[CrossRef](#)] [[PubMed](#)]
3. Wang, Y.; Cui, H.; Li, K.; Sun, C.; Du, W.; Cui, J.; Zhao, X.; Chen, W. A Magnetic Nanoparticle-Based Multiple-Gene Delivery System for Transfection of Porcine Kidney Cells. *PLoS ONE* **2014**, *9*, e102886. [[CrossRef](#)] [[PubMed](#)]
4. Zauner, W.; Farrow, N.; Haines, A. In vitro uptake of polystyrene microspheres: Effect of particle size, cell line and cell density. *J. Control. Release* **2001**, *71*, 39–51. [[CrossRef](#)]
5. Seemork, J.; Sansureerungsikul, T.; Sathornsantikun, K.; Sinthusake, T.; Shigyou, K.; Tree-Udom, T.; Jiangchareon, B.; Chiablaem, K.; Lirdpramongkol, K.; Svasti, J.; et al. Penetration of Oxidized Carbon Nanospheres through Lipid Bilayer Membrane: Comparison to Graphene Oxide and Oxidized Carbon Nanotubes, and Effects of pH and Membrane Composition. *ACS Appl. Mater. Interf.* **2016**, *8*, 23549–23557. [[CrossRef](#)] [[PubMed](#)]
6. Nakatsuji, H.; Numata, T.; Morone, N.; Kaneko, S.; Mori, Y.; Imahori, H.; Murakami, T. Thermosensitive Ion Channel Activation in Single Neuronal Cells by Using Surface-Engineered Plasmonic Nanoparticles. *Angew. Chem. Int. Ed.* **2015**, *54*, 11725–11729. [[CrossRef](#)] [[PubMed](#)]
7. Spindler, S.; Ehrig, J.; König, K.; Nowak, T.; Piliarik, M.; Stein, H.; Taylor, R.; Garanger, E.; Lecommandoux, S.; Alves, I.; et al. Visualization of lipids and proteins at high spatial and temporal resolution via interferometric scattering (iSCAT) microscopy. *J. Phys. D* **2016**, *49*, 274002. [[CrossRef](#)]
8. Zhang, S.; Gao, H.; Bao, G. Physical Principles of Nanoparticle Cellular Endocytosis. *ACS Nano* **2015**, *9*, 8655–8671. [[CrossRef](#)] [[PubMed](#)]
9. Morlot, S.; Roux, A. Mechanics of Dynamin-Mediated Membrane Fission. *Annu. Rev. Biophys.* **2013**, *42*, 629–649. [[CrossRef](#)] [[PubMed](#)]
10. Morlot, S.; Galli, V.; Klein, M.; Chiaruttini, N.; Manzi, J.; Humbert, F.; Dinis, L.; Lenz, M.; Cappello, G.; Roux, A. Membrane Shape at the Edge of the Dynamin Helix Sets Location and Duration of the Fission Reaction. *Cell* **2012**, *151*, 619–629. [[CrossRef](#)] [[PubMed](#)]
11. Pucadyil, T.; Schmid, S. Real-time visualization of dynamin-catalyzed membrane fission and vesicle release. *Cell* **2008**, *135*, 1263–1275. [[CrossRef](#)] [[PubMed](#)]
12. Roux, A.; Uyhazi, K.; Frost, A.; Camilli, P. GTP-dependent twisting of dynamin implicates constriction and tension in membrane fission. *Nature* **2006**, *441*, 528–531. [[CrossRef](#)] [[PubMed](#)]
13. Arayachukiat, S.; Seemork, J.; Pan-In, P.; Amornwachirabodee, K.; Sangphech, N.; Sansureerungsikul, T.; Sathornsantikun, K.; Vilaivan, C.; Shigyou, K.; Pienpinijtham, P.; et al. Bringing Macromolecules into Cells and Evading Endosomes by Oxidized Carbon Nanoparticles. *Nano Lett.* **2015**, *15*, 3370–3376. [[CrossRef](#)] [[PubMed](#)]
14. Shigyou, K.; Nagai, K.; Hamada, T. Lateral Diffusion of a Submicrometer Particle on a Lipid Bilayer Membrane. *Langmuir* **2016**, *32*, 13771–13777. [[CrossRef](#)] [[PubMed](#)]
15. Levin, Y.; Idiart, M. Pore dynamics of osmotically stressed vesicles. *Phys. A* **2004**, *331*, 571–578. [[CrossRef](#)]
16. Koster, G.; VanDuijn, M.; Hofs, B.; Dogterom, M. Membrane tube formation from giant vesicles by dynamic association of motor proteins. *Proc. Natl. Acad. Sci. USA* **2003**, *100*, 15583–15588. [[CrossRef](#)] [[PubMed](#)]
17. Angelova, M.; Dimitrov, D. Liposome electroformation. *Faraday Discuss. Chem. Soc.* **1986**, *81*, 303. [[CrossRef](#)]
18. Rawicz, W.; Olbrich, K.C.; McIntosh, T.; Needham, D.; Evans, E. Effect of Chain Length and Unsaturation on Elasticity of Lipid Bilayers. *Biophys. J.* **2000**, *79*, 328–339. [[CrossRef](#)]

